Atomic-Scale Analysis of the Oxygen Configuration at a $SrTiO_3$ Dislocation Core

C. L. Jia,* A. Thust, and K. Urban

Institute of Solid State Research and Ernst Ruska-Centre for Microscopy and Spectroscopy with Electrons (ER-C), Research Centre Jülich, D-52425 Jülich Germany

(Received 22 July 2005; published 22 November 2005)

The atomic structure of a $SrTiO_3$ dislocation is revealed directly by phase-retrieval electron microscopy. In particular, atomic columns of light oxygen are observed simultaneously with the columns of considerably heavier Sr and Ti. A distinct structural modification of the oxygen octahedra at the dislocation core as well as a significant nonstoichiometry, including a deficiency of oxygen, are observed. Deviations from the bulk chemical concentration are quantified column by column by means of structure modeling and quantum-mechanical simulations of the electron scattering process.

DOI: 10.1103/PhysRevLett.95.225506 PACS numbers: 61.72.Ff, 42.30.Rx, 68.37.Lp, 77.84.Bw

Dislocations, which appear almost unavoidably in many materials, have been at the focus of materials research for a long time. The mechanical behavior of elementary metals or alloys is strongly determined by the specific structure and kinetics of dislocations. Additionally, the electrical properties of functional materials applied in electronics depend crucially on the density and nature of the dislocations involved [1,2]. The structure and the kinetic behavior of dislocations in metals and semiconductors which have a simple crystal structure are well understood owing to extensive long-term research performed in the past. However, dislocation structures in oxides, especially in perovskite oxides, which play a key role in industrial nanoelectronics [3], are still not well-known due to their intrinsic structural and chemical complexity.

Perovskites are commonly described by the chemical formula ABO_3, where A represents cations with large radius, B stands for cations with small radius, and O denotes oxygen. A characteristic subunit of the perovskite structure is an octahedron formed by six oxygen atoms, which fills the three-dimensional space by mutually sharing corners. Geometrical alterations related to these octahedra, such as distortion and tilt, create a huge number of different structures and subsequently different materials properties [4]. $SrTiO_3$, the most prominent representative of the perovskite family, is a dielectric with a simple cubic unit cell. It has been shown that a deviation in stoichiometry, especially in the concentration of oxygen at defects, and in geometry (lattice distortion) may induce additional electrical properties such as conductivity [5] and ferroelectricity [6]. Therefore, the dislocations, which are at the focus of the present work, are also expected to have a similarly important influence on the measured macroscopic properties due to the related local lattice distortion, a possible structure change and a possible chemical anomaly. The knowledge of such defects thus serves as a guideline for the improvement of oxide materials with respect to their successful application in electronic devices. However, the ability to determine the geometrical and chemical distribution of light anions with atomic resolution in the presence of heavy cations has been so far an unsolved challenge in microstructure research.

High-resolution transmission electron microscopy (HRTEM) has proven to be a powerful tool for the characterization of lattice defects. The recently developed technique of the hardware correction of the spherical aberration (C_S) of the objective lens allows one to extend the point resolution of a microscope with field emission gun up to its information limit [7]. Moreover, a negative-C_S-imaging (NCSI) technique has recently been developed in our group using such a hardware corrector. With this novel imaging technique it is possible to image chemical elements with low nuclear charge such as oxygen with a comparatively higher contrast, which is especially useful in cases where the atoms are situated at a very close distance to strongly scattering heavy atoms [8–10].

An alternative HRTEM technique going beyond the pure correction of the spherical aberration is the numerical reconstruction of the quantum-mechanical electron exit-plane wave function using a focal series of images [11,12]. This technique has been applied successfully in the past for solving a variety of challenging defect structures on an atomic scale [13–16]. The benefit of using this technique in addition to the hardware correction of the spherical aberration is twofold in the present context. First, by the use of typically 20 different images with redundant information as input for the reconstruction procedure one achieves a considerable increase of the signal-to-noise ratio in the finally retrieved wave function compared to a single-shot image [17]. The implicit averaging over many images compensates for the high image noise caused by unstable and fluctuating amorphous cover layers on the specimen surfaces. Second, defocus and various unwanted residual aberrations of the objective lens, like twofold and threefold astigmatism or axial coma, which may blur the defect images and which cannot be kept satisfactorily constant during the experiment, can be determined *a posteriori* and numerically removed from the retrieved wave function [18,19].

In the present work, we take advantage of the two abovementioned techniques for investigating the atomic structure of a dislocation core in $SrTiO_3$. The emphasis of this investigation is not only on the spatial arrangement of the heavy cations Sr and Ti but also on the detailed arrangement of the considerably lighter oxygen atoms.

[110] oriented specimens for the HRTEM investigation were prepared from a single crystal of $SrTiO_3$ by a standard procedure including grinding, dimpling, and final ion-beam milling in a stage cooled with liquid nitrogen. Twenty images of a dislocation were recorded under NCSI conditions ($C_S = -40$ μm) with a nominal focal step size of -1.8 nm in the Philips CM200 FEG microscope equipped with a C_S corrector. Before recording the image series, the residual aberrations of the lens system were estimated by the evaluation of Zemlin tableaus taken of an amorphous image region with beam tilts up to 20 mrad [20]. These aberrations were reduced accordingly before experimental data acquisition by adjusting the appropriate lens currents of the C_S correction system. The exit-plane wave function was retrieved from the recorded image series using the Philips–Brite-Euram software package for focal-series reconstruction [11,12], which is also the basis of the TRUEIMAGE software [21]. The modeling of the core structure and the simulations of the wave function and images required for the subsequent quantitative comparisons were carried out with the CRYSTALKIT and MACTEMPAS software packages [22].

The actual experimental defocus values of the images in the series as well as the residual twofold astigmatism common to all images were determined using the reconstruction software. The focal values were found to lie in the interval between $+22$ and -9 nm, with a well-defined linear relationship between the focal values and the image numbers, yielding an actual focal step size of -1.62 ± 0.02 nm. The modulus of the residual twofold astigmatism was found to be as small as 0.9 nm.

Figure 1(a) displays image No. 9 belonging to a series of high-resolution images containing a dislocation core. This image was recorded at a defocus value of $+8.8$ nm, which is close to the optimum phase contrast under NCSI conditions [9]. In this image all types of atomic columns, i.e., SrO, Ti, and O, are directly revealed by bright dots on a dark background, as is marked by circles in the periodic lattice area. The arrows denote the dislocation with a Burgers vector $a[001]$. Whereas the cation columns in the core area can be identified in a quite straightforward manner from the C_S corrected image, the contrast of the oxygen columns is buried in comparatively strong noise. Moreover, the residual isotropic delocalization of 0.08 nm, which is unavoidably present under ideal phase-contrast conditions [9], together with the unwanted anisotropic residual aberrations, additionally hampers the identification of oxygen columns directly at the dislocation core. Figure 1(b) shows the corresponding phase image retrieved from the focal series of 20 images, which is delocalization-free due to an additional *a posteriori* elimination of all residual aberrations. In addition to the removal of the isotropic aberrations, defocus, and spherical aberration which are responsible for the unavoidable 0.08 nm phase-contrast delocalization, the anistropic aberrations removed were a twofold astigmatism of 0.9 nm, a threefold astigmatism of 70 nm and an axial coma of 50 nm. The details of the oxygen arrangement at the dislocation core are sufficiently well resolved after the numerical reconstruction and can now be studied column by column. From Fig. 1(b) it is clearly seen that the dislocation is characterized by the termination of two atomic planes, a (001) SrO plane and a (001) TiO_2 plane. The core area extends over about 0.8 nm, one and a half [110] periods between the different termination points of these two atomic planes. At this distance two Ti-O planes directly face each other, forming a structure of double Ti-O planes. This structure can be also considered as a short-distance dissociation of the dislocation.

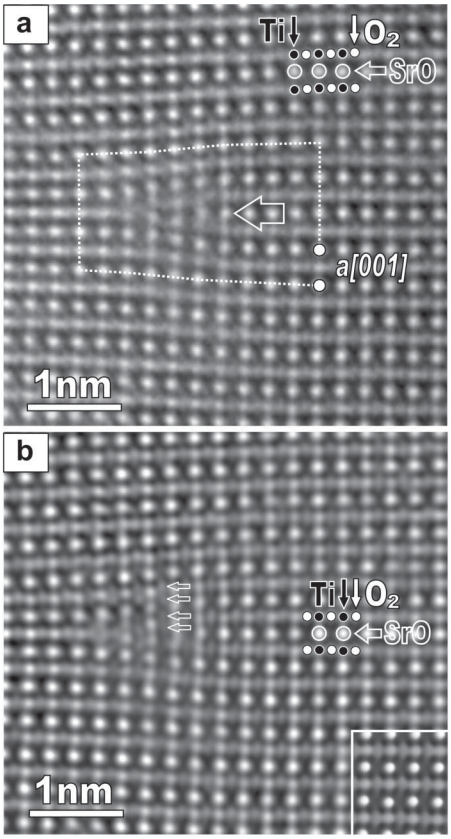

FIG. 1. (a) Image No. 9 belonging to a focal series of 20 images containing a dislocation core in [110] oriented $SrTiO_3$. The image was recorded with a value of the spherical aberration of -40 μm and a defocus value of $+8.8$ nm. Circles denote the atomic columns of SrO, Ti, and O. The Burgers circuit yields a Burgers vector $a[001]$. (b) Numerically retrieved phase from the same region after elimination of residual aberrations. The inset in the periodic area shows the simulated phase for a sample thickness of 4.3 nm. Pairs of arrows highlight the splitting of oxygen columns.

In order to determine the atomic configuration of the core structure and to estimate possible chemical concentration variation at the dislocation core, the sample thickness was determined first. Being aware of a possible local variation of the sample thickness, an image area at the bottom right of Fig. 1(b) was selected as a reference. Simulations of exit-plane wave functions belonging to the perfect lattice were carried out for all sample thickness values in question, including a small crystal tilt which was determined from slight asymmetries in the ideally centrosymmetric Fourier transform of the wave function [19]. For the selected reference area the best match between simulation, shown as the inset at the bottom right of Fig. 1(b), and experiment was found for a sample thickness of 4.3 nm through a quantitative comparison of the phase belonging to the SrO, the Ti, and the O atom columns. In considering the well-known contrast mismatch problem between experimental and simulated images [23], which also appears in comparisons between simulated and experimental wave functions, a single multiplicative constant was applied in order to adjust the contrast of simulated and experimental wave functions to the same level, as was previously done for image comparison [10].

The most prominent feature of the oxygen signal in the core region is a doubling of the phase maxima, as is marked by two pairs of small horizontal arrows in Fig. 1(b). Moreover, the phase peaks at the oxygen positions in the core region are in general considerably lower than those in the surrounding perfect lattice. Extensive simulations showed that the prominent doubling of phase maxima cannot be caused by a single column of oxygen, indicating that, indeed, two oxygen columns are responsible for the observed maximum doubling. A corresponding structure model was set up and further refined by adjusting the occupancy of the atomic columns in order to obtain as small a discrepancy as possible between simulated and experimentally retrieved phase. Figure 2(a) displays the simulated phase image of the dislocation core based on the refined structure model. For direct comparison, Fig. 2(b) displays the experimentally retrieved phase image of the core area. It is already obvious from visual inspection that the details of the phase images displayed in Figs. 2(a) and 2(b) mutually match each other to a high degree. Since a direct proportionality between the atomic occupancy of the columns and the phase values is confirmed by simulations, a more quantitative comparison based on the specific shape of phase profiles, which can be regarded as a direct structural fingerprint of the core region, was carried out. Phase profiles along five selected $(1\bar{1}0)$ planes in the core area are displayed below the corresponding phase images of Fig. 2. The excellent resemblance between the experimental and the simulated phase profiles supports in detail the validity of the refined structure model of the dislocation core.

Figure 3(a) shows the structure model of the dislocation core viewed along the [110] direction, where the occupancy deviation of the atomic columns is represented by the violet and red segments. The deviation levels are given

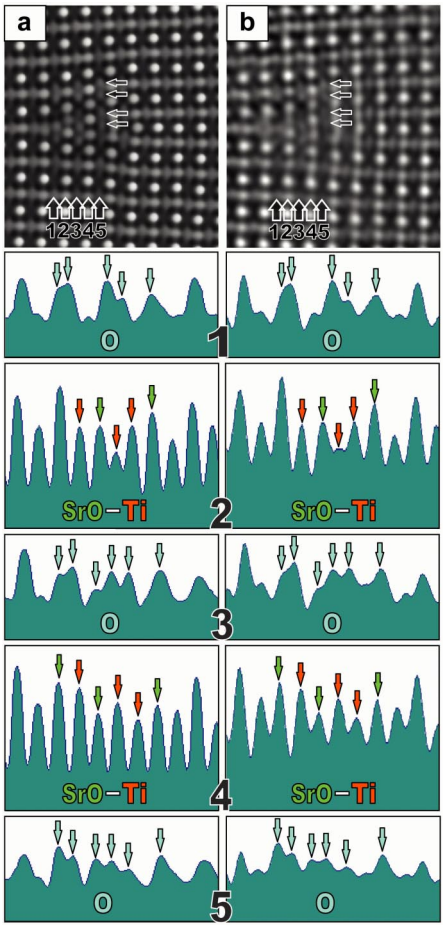

FIG. 2 (color online). Comparison between (a) the simulated phase image based on the structure model shown in Fig. 3 and (b) the phase image retrieved numerically from experimental data. Phase profiles along the atomic planes indicated by the numbered arrows in (a) and (b) demonstrate an excellent quantitative match between simulation and experiment.

with respect to a fully occupied column with a height of 4.3 nm. From our comparisons based on the perfect lattice we estimate the error in the given occupancy values to be around 5%. The decrease of the oxygen occupancy to around 50% right at the core region is perfectly consistent with the observation of the phase-peak doubling, suggesting that oxygen columns of the ideal structure are split into two semioccupied columns with a relative displacement in the [001] direction (vertical direction within the image plane). It is reasonable to assume that the column splitting occurs in such a way that the oxygen atoms undergo alternatively a mutually opposite shift relative to the ideal single-column position. This shift distorts the oxygen octahedra in the way denoted by solid lines in the structure model of Fig. 3(a). This distortion enables the arrangement of a modified polyhedron (or capped trigonal prism) involving seven oxygen atoms instead of six in the octahedron of the perfect periodic lattice. Figure 3(b) schematically shows the modification details of the octahedra at the dislocation core in a perspective view.

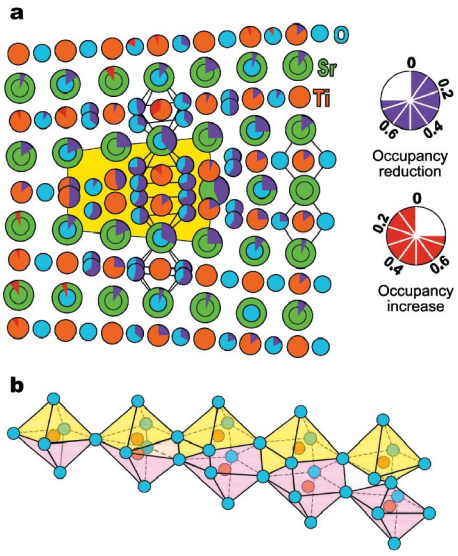

FIG. 3 (color). (a) Structure model of the dislocation core refined by matching the simulated phase to the experimentally retrieved phase. The violet segments at the atomic columns indicate the occupancy reduction relative to a fully occupied reference column of 4.3 nm height. The red segments indicate a slight formal over-occupancy due to experimental noise and local thickness variations with respect to the reference level. (b) Perspective view of the oxygen configuration at the dislocation core.

From the refinement of the structure model, it is found that most of the columns in the core region have a tendency to be under-occupied. This holds for the cation columns, which have occupancies slightly less than 1, as well as for the oxygen columns with occupancy values less than the ideal value 0.5 related to the column splitting. This finding might also indicate that the object thickness at the dislocation core could in general be lower than the thickness of the surrounding bulk material. Such a local thickness decrease could be caused by preferential thinning effects during ion-beam sample preparation. In this instance the detected low occupancy of the columns at the dislocation core could not be solely attributed to the existence of atomic vacancies. It is, however, important to state that a relative comparison of occupancies between various columns is still valid, even in the presence of a possible local thickness decrease. One can therefore calculate a relative occupancy ratio, i.e., the ratio between the number of cation atoms and oxygen atoms for neighboring atom columns. In the region of the dislocation core marked by the yellow background color, one obtains the atom ratio of 0.51:1.00:2.29 for Sr:Ti:O. In comparison to the stoichiometry of the $SrTiO_3$ the core is thus Sr and O deficient. It is known that the concentration of cations can vary for different dislocation types [9,24]. The direct observation of oxygen deficiency agrees well with the results obtained by other techniques [24]. The relatively low concentration of oxygen could result in a positively charged dislocation core.

Our results demonstrate that the combination of the hardware correction of the spherical aberration with numerical phase-retrieval techniques is a very powerful approach for atomic-scale structure investigations in HRTEM. This approach allowed us to reveal simultaneously the detailed atomic arrangement of cations and anions at a dislocation core in $SrTiO_3$. By the subsequent comparison of the experimentally acquired and processed data with simulations based on various structure models the geometrical and chemical details of the dislocation core could be determined at an atomic level, providing a complete structural data basis, which can be used as a starting point for calculations of the electronic properties of such defects.

*Email address: c.jia@fz-juelich.de

[1] M.-W. Chu *et al.*, Nat. Mater. **3**, 87 (2004).
[2] S. P. Alpay, I. B. Misirlioglu, V. Nagarajan, and R. Ramesh, Appl. Phys. Lett. **85**, 2044 (2004).
[3] N. Setter and R. Waser, Acta Mater. **48**, 151 (2000).
[4] O. Bock and U. Müller, Acta Crystallogr. Sect. B **58**, 594 (2002).
[5] K. Szot, W. Speier, R. Carius, U. Zastrow, and W. Beyer, Phys. Rev. Lett. **88**, 075508 (2002).
[6] J. H. Haeni *et al.*, Nature (London) **430**, 758 (2004).
[7] M. Haider *et al.*, Nature (London) **392**, 768 (1998).
[8] C. L. Jia, M. Lentzen, and K. Urban, Science **299**, 870 (2003).
[9] C. L. Jia, M. Lentzen, and K. Urban, Microsc. Microanal. **10**, 174 (2004).
[10] C. L. Jia and K. Urban, Science **303**, 2001 (2004).
[11] W. M. J. Coene, A. Thust, M. Op De Beeck, and D. Van Dyck, Ultramicroscopy **64**, 109 (1996).
[12] A. Thust, W. M. J. Coene, M. Op De Beeck, and D. Van Dyck, Ultramicroscopy **64**, 211 (1996).
[13] R. Rosenfeld, A. Thust, W. Yang, M. Feuerbacher, and K. Urban, Philos. Mag. Lett. **78**, 127 (1998).
[14] C. L. Jia and A. Thust, Phys. Rev. Lett. **82**, 5052 (1999).
[15] C. Kisielowski *et al.*, Ultramicroscopy **89**, 243 (2001).
[16] S. H. Yang, L. Croguennec, C. Delmas, E. C. Nelson, and M. O'Keefe, Nat. Mater. **2**, 464 (2003).
[17] A. Thust and R. Rosenfeld, *Proceedings of the 14th International Congress on Electron Microscopy* (Institute of Physics Publishing, Bristol and Philadelphia, 1998), p. 119.
[18] A. Thust, M. Overwijk, W. Coene, and M. Lentzen, Ultramicroscopy **64**, 249 (1996).
[19] A. Thust, C. L. Jia, and K. Urban, Microsc. Microanal. **9**, 140 (2003).
[20] S. Uhlemann and M. Haider, Ultramicroscopy **72**, 109 (1998).
[21] TRUEIMAGE is a commercial software package distributed by the FEI Company.
[22] M. A. O'Keefe and R. Kilaas, Scanning Microsc., Suppl. **2**, 225 (1988).
[23] M. J. Hÿtch and W. M. Stobbs, Ultramicroscopy **53**, 63 (1994).
[24] Z. Zhang, W. Siegle, and M. Rühle, Phys. Rev. B **66**, 094108 (2002).